第十一屆全國機構與機器設計學術研討會　　明新科技大學　台灣、新竹
中華民國九十七年十一月十四日　　論文編號：　A1N-23931

Design of a Training and Rehabilitation Upper Limb Exoskeleton without Actuators for Hemiperatic Stroke Patients

Po-Yang Lin[1]　Win-Bin Shieh[2]　Dar-Zen Chen[3,*]

[1]Dept. of Mechanical Engineering, National Taiwan University, Taipei, Taiwan
[2]Dept. of Mechanical Engineering, Mingchi University of Technology, Taipei, Taiwan
[3]Dept. of Mechanical Engineering, National Taiwan University, Taipei, Taiwan

Abstract

This paper presents a design of an upper limb exoskeleton for rehabilitation and training. The device consists of three zero-free-length springs which compensate the weight of the patient's upper limb during its full range of motion. It provides a gravity-reduced environment and assists a patient performing the training exercises on his/her own control. The design which consists of no actuating motors is simpler and less expensive, but with similar benefits as other therapeutic robots. A model of this design was tested in computer simulation and demonstrates the achievement based on movements of upper limb of activities of daily livings.

Keywords: upper limb exoskeleton, gravity balance, robotic therapy, activity of daily livings

1. Introduction

In the United States more than 700,000 people suffer a stroke each year [1], and approximately two-thirds of these individuals survive and require rehabilitation. The goals of rehabilitation are to help survivors become as independent as possible and to attain the best possible quality of life.

Paralysis is one of the most common disabilities resulting from stroke. The paralysis is usually on the side of the body opposite the side of the brain damaged by stroke, and may affect the face, an arm, a leg, or the entire side of the body. This one-sided weakness is called hemiparesis. Stroke patients with hemiparesis may suffer from muscular weakness and have difficulty with everyday activities such as walking, raising arm or grasping objects. Physical therapists help survivors regain the use of stroke-impaired limbs, teach compensatory strategies to reduce the effect of remaining deficits, and establish ongoing exercise programs to help people retain their newly learned skills. Disabled people tend to avoid using impaired limbs, a behavior called "learned non-use". The repetitive use of impaired limbs encourages brain plasticity and helps reduce disabilities.

"Passive" range-of-motion exercises are those in which the therapist actively helps the patient move a limb repeatedly, whereas "active" exercises are performed by the patient with no physical assistance from the therapist. The torque of a human joint during a typical movement can be broken down into gravity torque, inertia torque and muscular compliance torque [5]. In rehabilitation, at slow motion is expected, the dominance is the gravity torque. In this paper, the goal is to design a "semi-passive" rehabilitation device allowing stroke patient conduct upper limb movements on his/her own control in a provided gravity-reduced environment. The "semi-passive" device assists a patient performing the exercises in the same time requiring his/her own active control.

Robot-assisted movement training improves arm movement ability following acute and chronic stroke. Since 1997 the pioneering study of Massachusetts Institute of Technology MIT-Manus [8], numerous researchers have been developing robot-assisted therapeutic devices, i.e. the ARM-guide [9], MAHI exoskeleton [7], CADEN-7 [10], etc. Initial results are promising: patients who receive more therapy with a robotic device recover more movement ability. Efforts toward developing robotic treatment are motivated by the increasing public health burden associated with stroke-related disability and the current emphasis on cost reduction in health care that has resulted in shorter in patient rehabilitation of stay. Lum, P. S., et. al (2002) made a comparison of the robot-assisted with the conventional therapy [24]. Study shows that, in most aspects, robot-assisted therapy benefits from its highly repetitive exercise and precise quantitative need to a specific subject. For example, the robot-assisted device can progressively and precisely reduces assistance as the subject improved, and applies minimal assistance or even resistance to movement for mildly impaired subjects. However, most robotic rehabilitation devices are actively actuated. L. E. Kahn et. al. (2006) even put

* Corresponding author, e-mail: dzchen@ccms.ntu.edu.tw

a key question: “Is the expense of an actuated device needed to achieved therapeutic benefit? ” [14], or putting it another way, “Could similar benefits be achieved with simpler, less-expense, non-robotic technology that facilitates movement practice?” Rahmen, T. et al. (2007) had proposed a gravity-reduced device, the WREX, for retraining the upper limb movements [2]. The element for gravity reduction in WREX is constituted by elastic bands connected to parallel auxiliary links. The model for this exoskeleton is generally a planar two-DOF serial linkage. A universal joint is applied to each joint which allows two extra DOFs. This design provides an alternative solution to a non-actuated robotic therapeutic device. However, still, this model has limited range-of-motion comparing to a human upper limb. And fully gravity balance can only be achieved when arm and forearm are both situated on a vertical plane. The T-WREX is a modified version of the WREX [3]. The system is embedded of a grip sensor and software that simulates functional activities. The T-WREX has larger workspace comparing to the WREX. And it modeled the elbow as a 3-DOF joint. However, compensation of gravity effects is still limited. Although the systems of WREX and T-WREX consist no actuating motor, experiments had shown the passively gravity-reduction made progress in rehabilitation of patients with impaired limbs. Agrawal, S. K. et al. (2007) also implemented the gravity balancing techniques in a leg orthosis for gait training rehabilitation [4, 5]. This orthosis following the lower extremity is also considered as a planar two-link serial linkage. And it utilizes the parallel auxiliary links as well to locate the system center of mass and places the springs to suitable position that they can completely balance the effect of gravity over the range of motion. However, the orthosis can balance the lower extremity only in the swing motion.

Summing-up, a gravity-reduced rehabilitation machines without actuating motors are usually accomplished by elastics or springs [2-5]. Relative theories about gravity balancing multi-DOF linkages utilizing spring elements are studied by many engineers [11-13]. In order to provide suitable spring attachment points, most of the designs added parallel auxiliary links to the linkage. For spatial linkages, adding auxiliary links complicates the mechanism. Such method may be impractical in designing a wearable device for upper limb due to the interferences between the auxiliary links and the upper limb. In this paper, a novel spring balancing method is proposed without the parallel auxiliary links. Direct spring attachments are proved capable of balancing the weights of an upper limb combining the exoskeleton. Also, in our design, the constraint force acted on a subject is inherited from the weight of his/her upper limb instead of an actively actuated force constraint like other robotic rehabilitation systems. This is a safer and a more comfortable design.

2. Kinematic modeling of upper limb

2.1 Kinematic model

As in Fig. 1, an upper limb includes two segments, the upper arm and the forearm, where the upper arm is the region from the shoulder *S* to the elbow *E*, and the forearm is from the elbow *E* to the fingertip *F*. The main objective of the rehabilitation device is to reduce the torques acting on the joints of shoulder and elbow due to the weights of the upper arm and the forearm. And since the mass of human hand is relatively small comparing to the upper arm and forearm, the gravitational variation due to the wrist motion is negligible. At any instantaneous moment during the upper limb movements, the hand is at its neutral position. The relative positions of mass centers M_u and M_f with respect to the upper arm and the forearm are assumed fixed and always locate on their corresponding center lines. Therefore, the upper limb combining the exoskeleton can be modeled as a two link serial linkage, the arm-link and forearm-link.

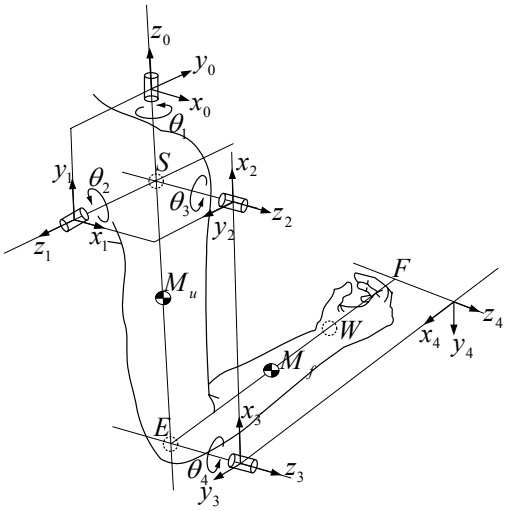

Fig. 1 Kinematics and coordinate systems for a right upper limb

The shoulder joint is equivalent to a 3-DOF ball joint. And since the forearm is generally axial symmetry, the forearm pronation-supination has little effect on the total variation of the gravity torques. The elbow joint is modeled as a 1-DOF joint allowing only the flexion-extension. The motion about the shoulder joint is complicated. For years, it has no unified descriptions. Some studies [10, 15-17] described the arm rotation about the shoulder joint by the Euler rotation angle. Similar concept broadly used in robotic kinematics is the Denavit-Hartenberg (D-H) transformation matrix. A. A. Hussein et. al (2006) proposed a biomechanical

model based on the D-H matrix method for assessing and monitoring the upper limb therapy [20].

The overall 4-DOF model of the upper limb is established as in Fig. 1. Following Denavit and Hertenberg's convention (1955), four Cartesian coordinate systems (CSs), CS 1, 2, 3 and 4, are attached to each link and CS 0 is attached to ground. The 4×4 homogenous transformation matrix is

$$ {}^{i-1}\boldsymbol{T}_i = \begin{pmatrix} \cos\theta_i & -\cos\alpha_i\sin\theta_i & \sin\alpha_i\sin\theta_i & a_i\cos\theta_i \\ \sin\theta_i & \cos\alpha_i\cos\theta_i & -\sin\alpha_i\cos\theta_i & a_i\sin\theta_i \\ 0 & \sin\alpha_i & \cos\alpha_i & d_i \\ 0 & 0 & 0 & 1 \end{pmatrix} \quad (1) $$

where θ_i's are the joint variables.

Since the origins of CSs 0, 1, 2 are coincident at point *S*, their corresponding d_i and a_i are zeros. The D-H parameters are listed in Table 1 where r_{SE} is the segmental length of the upper arm measured from the shoulder pivot to the elbow pivot, and r_{EF} is the segmental length of the forearm measured from the elbow pivot to the fingertip. Basically, the motion of a upper limb can be categorized into five motions; shoulder internal-external rotation θ_1, shoulder abduction-adduction θ_2, shoulder flexion-extension θ_3 and elbow flexion-extension θ_4 about the z_0, z_1 and z_2 axes, respectively [10, 16, 19].

Table 1. D-H parameters for a right upper limb

Frame *i*	d_i	θ_i	a_i	α_i
1	0	θ_1	0	90°
2	0	θ_2	0	90°
3	0	θ_3	$-r_{SE}$	0
4	0	θ_4	$-r_{EF}$	0

2.2 Gravity torques on the modeled joints

The gravitational potential energy of the upper limb is

$$ \begin{aligned} V_g &= -m_u \boldsymbol{g}\cdot\boldsymbol{r}_{SM_u} - m_f \boldsymbol{g}\cdot\boldsymbol{r}_{SM_f} \\ &= -m_u(-g\boldsymbol{k_0})\cdot(-r_{SM_u}\boldsymbol{i_3}) \\ &\quad -m_f(-g\boldsymbol{k_0})\cdot(-r_{SE}\boldsymbol{i_3} - r_{EM_f}\boldsymbol{i_4}) \end{aligned} \quad (2) $$

where m_u and m_f are the segmental masses of the upper arm and forearm, respectively. And r_{SMu} and r_{EMf} are the distances from the shoulder joint and the elbow joint to the segmental mass centers M_u and M_f, respectively.
Derived from the D-H transformation matrix, for CS 0 with respect to CS 2,

$$ \boldsymbol{k_0} = (\sin\theta_2)\boldsymbol{i_2} + (-\cos\theta_2)\boldsymbol{k_2} \quad (3) $$

And since $(\boldsymbol{k_2}\cdot\boldsymbol{i_3})$ and $(\boldsymbol{k_2}\cdot\boldsymbol{i_4})$ are zeros, insert Eq. (3) into (2) yields

$$ \begin{aligned} V_g &= (-m_u g r_{SM_u}\sin\theta_2 - m_f g r_{SE}\sin\theta_2)(\boldsymbol{i_2}\cdot\boldsymbol{i_3}) \\ &\quad +(-m_f g r_{EM_f}\sin\theta_2)(\boldsymbol{i_2}\cdot\boldsymbol{i_4}) \end{aligned} \quad (4) $$

For the system potential energy being *V*, the joint torque τ_i about each modeled joint *i* is

$$ \tau_i = \frac{\partial V}{\partial \theta_i}, \quad i = 1, 2, 3, 4 \quad (5) $$

Equation (5) suggests that the gravity torque of each joint is due to the configuration variant gravitational potential energy. The goal of our device is to achieve a constant system potential energy by adding the elastic potential energy opposite to the gravitational potential energy which the system suffers zero gravity effect.

3. Design assembly of the exoskeleton

An exposed view of the design of the exoskeleton wore on the upper limb is shown as Fig. 2. The three joint axes z_0, z_1 and z_2 are orthogonal and intersect on the center point *S* of the shoulder. Joints of axes z_i's are all revolute. And link 1 can be either pivoted about z_0 on a wearable shoulder pad or a grounded bench depending on its clinical requirements. Axes z_2 and z_3 are parallel. And the link length of link 3 is adjustable so that axis z_3 aligns with the joint axis of the elbow joint.

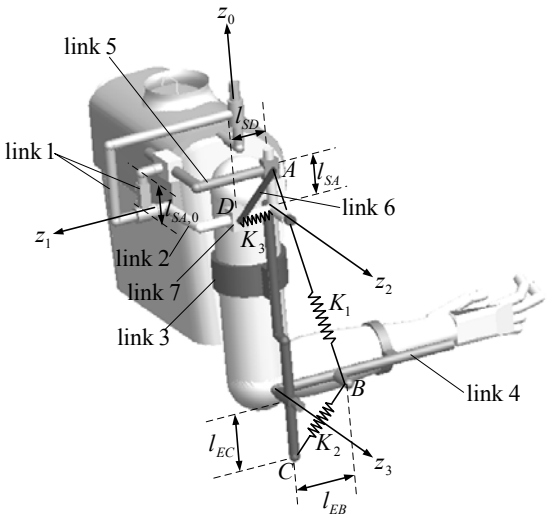

Fig. 2 An exposed view of the exoskeleton and spring connections

Links 3 and 4 are rigidly attached to the upper arm and the forearm, respectively. Serial linkage of links 1, 2, 3 and 4 generally follows the motions of the attached upper limb. Links 5 is allowed sliding along the x_2 axis of link 2. Its translational displacement is a pure sine function of rotation angle θ_2. Link 6 is in Cardanic motion with one end pivoted on link 5 and the other end sliding along the y_2 axis of link 2. For the balance of the weight of the upper limb, three coplanar-installed zero free length springs are attached to the exoskeleton. Spring K_1 is attached to point *A* on link 5 and point *B* on link 4, spring K_2 is attached to point *B* on link 4 and point *C* on link 3, and spring K_3 is attached to point *D* on link 6 and the intersecting point of axes x_2 and y_2 on link 2.

3.1 Spring design conditions

Since the three springs are coplanar. A schematic of the spring installations is illustrated as in Fig. 3. Corresponding elastic potential energies $V_{s,1}$, $V_{s,2}$ and $V_{s,3}$ of springs K_1, K_2 and K_3 are derived as

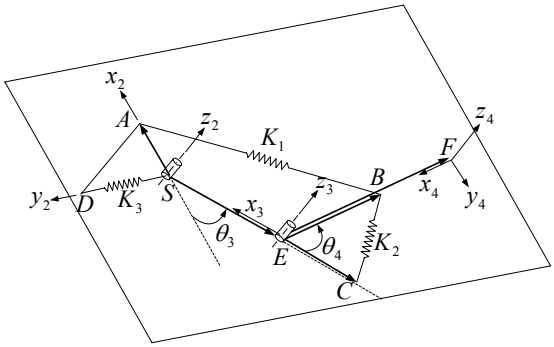

Fig. 3 Three co-planar installed zero-free-length springs

$$\begin{aligned} V_{s,1} &= \frac{1}{2}K_1(\boldsymbol{l_{AB}})\cdot(\boldsymbol{l_{AB}}) \\ &= \frac{1}{2}K_1(-r_{SE}\,\boldsymbol{i_3} - l_{EB}\,\boldsymbol{i_4} - l_{SA}\,\boldsymbol{i_2})\cdot(-r_{SE}\,\boldsymbol{i_3} \\ &\quad -l_{EB}\,\boldsymbol{i_4} - l_{SA}\,\boldsymbol{i_2}) \\ &= (K_1 r_{SE} l_{SA,0}\sin\theta_2)(\boldsymbol{i_2}\cdot\boldsymbol{i_3}) + (K_1 l_{EB} l_{SA,0}\sin\theta_2)(\boldsymbol{i_2}\cdot\boldsymbol{i_4}) \\ &\quad + (K_1 r_{SE} l_{EB})(\boldsymbol{i_3}\cdot\boldsymbol{i_4}) + \frac{1}{2}K_1(l_{SA,0}\sin\theta_2)^2 + const. \end{aligned} \tag{6}$$

$$\begin{aligned} V_{s,2} &= \frac{1}{2}K_2(\boldsymbol{l_{BC}})\cdot(\boldsymbol{l_{BC}}) \\ &= \frac{1}{2}K_2(-l_{EC}\,\boldsymbol{i_3} + l_{EB}\,\boldsymbol{i_4})(-l_{EC}\,\boldsymbol{i_3} + l_{EB}\,\boldsymbol{i_4}) \\ &= (-K_2 l_{EC} l_{EB})(\boldsymbol{i_3}\cdot\boldsymbol{i_4}) + const. \end{aligned} \tag{7}$$

and

$$\begin{aligned} V_{s,3} &= \frac{1}{2}K_3(l_{SD})^2 \\ &= \frac{1}{2}K_3({l_{AD}}^2 - {l_{SA}}^2) \\ &= -\frac{1}{2}K_3(l_{SA,0}\sin\theta_2)^2 + const. \end{aligned} \tag{8}$$

where $l_{SA,0}$ is the initial distance from points S to A. Summing Eqs. (4), (6), (7) and (8) yields the total potential energy as

$$\begin{aligned} V &= V_g + \sum_{i=1}^{3} V_{s,i} \\ &= (-m_u g r_{SM_u} - m_f g r_{SE} + K_1 r_{SE} l_{SA,0})(\sin\theta_2 \boldsymbol{i_2}\cdot\boldsymbol{i_3}) \\ &\quad + (-m_f g r_{EM_f} + K_1 l_{EB} l_{SA,0})(\sin\theta_2 \boldsymbol{i_2}\cdot\boldsymbol{i_4}) \\ &\quad + (K_1 r_{SE} l_{EB} - K_2 l_{EC} l_{EB})(\boldsymbol{i_3}\cdot\boldsymbol{i_4}) \\ &\quad + \frac{1}{2}(K_1 - K_3)(l_{SA,0})^2(\sin\theta_2)^2 + const. \end{aligned} \tag{9}$$

Setting the coefficient of each configuration variant term zero, the spring design conditions can be obtained as

$$l_{SA,0} = \frac{m_u g r_{SM_u} + m_f g r_{SE}}{K_1 r_{SE}} \tag{10a}$$

$$l_{EB} = \frac{m_f r_{EM_f} r_{SE}}{m_u r_{SM_u} + m_f r_{SE}} \tag{10b}$$

$$l_{EC} = \frac{K_1}{K_2} r_{SE} \tag{10c}$$

and

$$K_3 = K_1 \tag{10d}$$

As the patient progressing during the rehabilitation process, his/her upper limb can produce larger joint torques and requires less aid from the exoskeleton. The exoskeleton may decrease its level of gravity-reduction proportionally. 100% of gravity-reduction is referred to the zero gravity environment in which the patient requires zero effort against the gravity torques on the shoulder and elbow. From the spring conditions, if the desired percentage p% of the weight, equivalently p% gravity-reduced environment, is to be balanced, the spring conditions can be obtained by replacing the mass parameters m_u (or m_f) with $(p\%)m_u$ (or $(p\%)m_f$) in Eqs. (10). As a result, only Eq. (10a) needs to be modified as

$$l'_{SA,0} = (p\%)\frac{m_u g r_{SM_u} + m_f g r_{SE}}{K_1 r_{SE}} \tag{11}$$

As in Fig. 2, by adjusting the initial crank length $l_{SA,0}$, different levels of gravity-reduction can be accomplished.

For an individual subject, the spring installation conditions must satisfy Eqs. (10) corresponding to the upper limb parameters. Changing of spring constants, K_1, K_2 and K_3, requires changes of the entire springs of the exoskeleton which is a more inconvenient task, rather than that, adjusting the spring attachment points can be preferable. The range of adjustment of a spring attachment point for different subjects can be relatively small if the springs used are stiff enough. Zero-free-length spring, in practice, can be done by combining a spring with "negative" length in which the coils press together when the spring is relaxed with an extra length of inelastic material. This type of spring was developed in 1932 by Lucien LaCoste for use in a vertical seismograph. Recently, many studies proposed several equivalent zero-free-length spring arrangements by non-zero-free-length springs combing cables and pulleys or alignment shafts [12, 13].

3.2 Anthropometric parameters of the upper limb

Based on the designs of springs and the exoskeleton, certain anthropometric parameters of the upper limb of the patient, who intends to use, has to be known for the adjustments of the device. The total body weight (TBW) and the link lengths, r_{SE} and r_{EF}, of the upper arm and the forearm can be measured easily and precisely in prior. By knowing this, the link length of link 3 can be

adjusted so that the axis z_3 of the exoskeleton aligned to the axis of elbow joint. Information of other parameters, e.g., the segmental weights of the upper limb, the locations of segmental mass centers, may be difficult to measure directly from a living patient. Prior studies [21-23] had proposed several regression equations for estimating the segmental weights of the upper limb and the corresponding locations of mass centers. These equations are derived from those easily obtained anthropometric input as independent variables. They have a relatively small standard error of estimate (ε). Data derived from these equations will be appropriate for the individualized models. The coefficients for the regression equations are listed in Table 2. The required upper limb parameters can be estimated accordingly as

$$m_u = .0274\times(\text{TBW}) - .01, \quad \varepsilon_{m_u} = .19 \tag{12a}$$

$$m_f = .0233\times(\text{TBW}) - .01, \quad \varepsilon_{m_f} = .20 \tag{12b}$$

$$\begin{aligned} r_{SM_u} + \Delta_s^* = {} & .329\times(\text{humerus rad. length}) \\ & - .25\times(\text{upper arm cir.}) \\ & + 2.827\times(\text{elbow breadth}) \\ & - 6.168, \quad \varepsilon_{SM_u} = .72 + \varepsilon_{\Delta_s} \end{aligned} \tag{12c}$$

and

$$\begin{aligned} r_{EM_f} = {} & 1.617\times(\text{wrist breadth}) \\ & - .585\times(\text{radiale-stylion length}) \\ & - .331\times(\text{forearm cir.}) + .510, \quad \varepsilon_{EM_f} = .46 \end{aligned} \tag{12d}$$

Table 2　Coefficients for the regression equations (data given in Kg, cm; Precise definition of all dimensions, see Clauser et. al. [23])

Segment		Independent regression variables			Constant	ε
Upper arm	Length (measured from Acromion)	Humerus rad. length	Upper arm circumference	Elbow breadth		
		.707			-4.563	1.21
		.710	-.045		-3.333	1.26
		.329	-.250	+2.827	-6.168	.72
	Mass	Total body weight				
		.0274			-.01	.19
Forearm	Length (measured from Radiale)	Wrist breadth	Radiale-Stylion length	Forearm circumference		
		2.765			+.405	.72
		1.962	+.379		-4.822	.62
		1.617	+.585	-.331	+.510	.46
	Mass	Total body weight				
		.0233			-.01	.20

Note that Δ_s^* in Eq. (12c) is the distance from the acromion to the shoulder pivot. Its mean value and estimated error, Δ_s^* and $\varepsilon_{\Delta s}$, are 3.8 cm and 0.2 cm, respectively [25]. Based on measuring the anthropometric parameters of a specified subject, required information of the upper limb of the subject is derived from Eqs. (12a-d) and listed in Table 4. The following simulation is based on this individualized model where the specific spring conditions are derived from Eqs. (10) and listed in Table 4. Note that the crank length $l_{SA,0}$ in Table 4 is designated for 100 % gravity-reduced condition.

Table 4　Spring design parameters and correspondent subject information

Subject anthropometric parameters	total body weight = 80 kg humerus rad. length = 33.2 cm radiale-stylion length = 27.1 cm upper arm cir. = 33.1 cm forearm cir. = 30.0 cm elbow breadth = 8.5 cm wrist breadth = 5.7 cm
Estimated upper limb parameters	r_{SE} : 28.60 cm m_u : 2.18 Kg m_f : 1.85 Kg r_{SM_u} : 16.71 cm r_{EM_f} : 15.65 cm
Spring design parameters	K_1 : 0.5 Kgw/cm K_2 : 1.5 Kgw/cm K_3 : 0.5 Kgw/cm $l_{SA,0}$: 6.25 cm l_{EB} : 9.27 cm l_{EC} : 9.53 cm

4. Activities of daily livings

In rehabilitation practices, a number of key activities, activities of daily livings (ADL), are generally defined that described the functional capacity of patients [15, 16]. Many function outcome scores commonly used in evaluation of the functional capacity of an upper limb is based on the ADL. One of the most important motions in ADL is the eating motion. This motion requires patient's upper limb to reach forward and bring the food to his/her mouth.

The model of the upper limb combining the exoskeleton is built in ADAMS, computer simulation software, and the following result should demonstrate the achievement of this design. The input motion of the upper limb is conducting an eating motion. The movements are defined by the joint angles, θ_1 , θ_2 , θ_3 and θ_4 , of the exoskeleton as in Figs. 6(a)-(d). The initial configuration of the upper limb is shown as Fig. 2 where the forearm is horizontal and the upper arm rests vertically.

Figures 7(a)-(c) plot the time history of the gravity torques about each modeled joint axis z_1, z_2, z_3 during the eating motion. The solid lines represent the original, unbalanced, gravity torques. It is observed that, of this movement, the maximum torques of shoulder abduction-adduction, flexion-extension and elbow flexion-extension are 6106, 5385 and 3244 N-mm, respectively. The dash lines represent the gravity torques in p% gravity-reduced environment achieving by the exoskeleton. Their corresponding crank length, $l_{SA,0}$, is (p%)(6.25) cm.

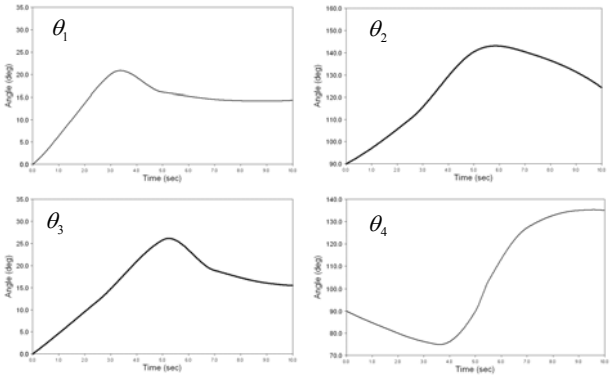

Fig. 6 The joint angles of a right upper limb of an eating motion

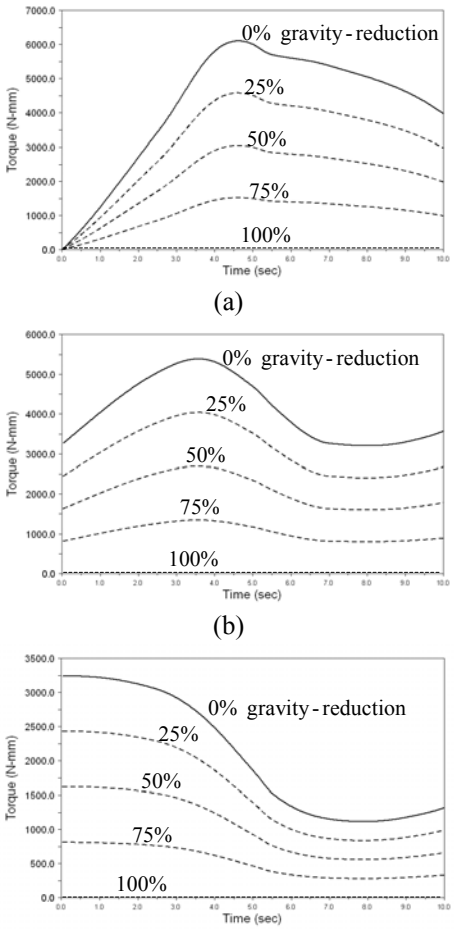

Fig. 7 Different levels of gravity-reduction and joint torques of (a) shoulder abd/add (b) shoulder flx/ext (c) elbow flx/ext

Note that, in 0% gravity-reduced environment, the balanced gravity torques are equal to that of the unbalanced ones. That is, with the initial installing length of spring 1 on the sliding yoke, $l_{SA,0}$, being zero, the length of spring 3 does not vary along the motion of upper limb. And the spring forces of springs 1 and 2 counteract each other. The gravity environment of the system with this particular spring installation is equivalent a system without springs.

5. Design errors due to anthropometric estimation

Although the adjustment of spring attachments can be customized for each individual subject, however still, it is based on the estimation of the segmental weights and locations of mass centers from the regression equations. Inaccurate level of gravity reduction may occur due to the estimated errors of the upper limb parameters. And since the device contains no external actuator and sensory controller, the sensitivity must be further investigated to ensure that the inaccuracies are tolerable.

By substituting the estimated errors of Eqs. (12) into Eq. (9), the estimated error of the total potential energy is

$$\begin{aligned}\varepsilon_V =&(-m_u\varepsilon_{SM_u}g-\varepsilon_{m_u}r_{SM_u}g-\varepsilon_{m_u}\varepsilon_{SM_u}g\\&-\varepsilon_{m_f}gr_{SE})\sin\theta_2\cos\theta_3+(-m_f\varepsilon_{EM_f}g-\varepsilon_{m_f}r_{EM_f}g\\&-\varepsilon_{m_f}\varepsilon_{EM_f}g)\sin\theta_2\cos(\theta_3+\theta_4)\end{aligned} \quad (13)$$

The estimated error of the gravity torque about each joint will be

$$\varepsilon_{\tau,1}=\frac{\partial\varepsilon_V}{\partial\theta_1}=0 \quad (14a)$$

$$\begin{aligned}\varepsilon_{\tau,2}=&\frac{\partial\varepsilon_V}{\partial\theta_2}\\=&(-m_u\varepsilon_{SM_u}g-\varepsilon_{m_u}r_{SM_u}g-\varepsilon_{m_u}\varepsilon_{SM_u}g\\&-\varepsilon_{m_f}gr_{SE})\cos\theta_2\cos\theta_3+(-m_f\varepsilon_{EM_f}g\\&-\varepsilon_{m_f}r_{EM_f}g-\varepsilon_{m_f}\varepsilon_{EM_f}g)\cos\theta_2\cos(\theta_3+\theta_4)\end{aligned} \quad (14b)$$

$$\begin{aligned}\varepsilon_{\tau,3}=&\frac{\partial\varepsilon_V}{\partial\theta_3}\\=&(m_u\varepsilon_{SM_u}g+\varepsilon_{m_u}r_{SM_u}g+\varepsilon_{m_u}\varepsilon_{SM_u}g\\&+\varepsilon_{m_f}gr_{SE})\sin\theta_2\sin\theta_3+(m_f\varepsilon_{EM_f}g\\&+\varepsilon_{m_f}r_{EM_f}g+\varepsilon_{m_f}\varepsilon_{EM_f}g)\sin\theta_2\sin(\theta_3+\theta_4)\end{aligned} \quad (14c)$$

and

$$\begin{aligned}\varepsilon_{\tau,4}=&\frac{\partial\varepsilon_V}{\partial\theta_4}\\=&(m_f\varepsilon_{EM_f}g+\varepsilon_{m_f}r_{EM_f}g\\&+\varepsilon_{m_f}\varepsilon_{EM_f}g)\sin\theta_2\sin(\theta_3+\theta_4)\end{aligned} \quad (14d)$$

In the case of the eating motion, 100% gravity reduction, the resultant gravity torques about each modeled joint axis z_1, z_2, z_3 based on the maximum estimated errors are shown in Figs. 8 (a)-(c), respectively. For shoulder abduction-adduction, flexion-extension and elbow flexion-extension, upon the possible maximum estimated errors of the upper limb parameters, the average levels of gravity reductions can still achieve 89.56%, 88.51% and 87.68%, respectively. The device has low sensitivity to the estimated errors of upper limb parameters and is considered relatively reliable.

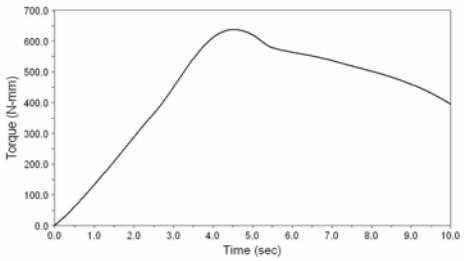

(a)

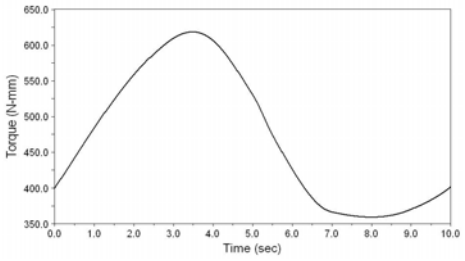

(b)

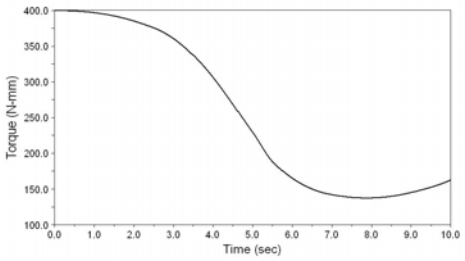

(c)

Fig. 8 The positive residual joint torques of (a) shoulder abd/add (b) shoulder flx/ext (c) elbow flx/ext due to maximum estimated errors

6. Conclusion

This paper presents a design of an upper limb exoskeleton for rehabilitation and training. The device consists three zero-free-length springs which compensate the weight of the patient's upper limb during its full range of motion. Detailed design parameters related to a subject's upper limb are given. Reliability and sensitivity of the device are further discussed. A model of this design was tested in computer simulation and demonstrates the achievement of gravity balance on the movement of an eating motion.

Reference

[1] American Stroke Association, 2005 [Online]. Available: http://www.strokeassociation.org/

[2] T. Rahman, W. Sample, R. Seliktar, M. T. Scavina, A. L. Clark, K. Moran, M. A. Alexander, "Design and Testing of a Functional Arm Orthosis in Patients with Neuromuscular Diseases," *IEEE Transactions on Neural Systems and Rehabilitation Engineering*, vol. 15, no. 2, pp. 244-251, June 2007.

[3] R. J. Sanchez, J. Liu, S. Rao, P. Shah, R. Smith, T. Rahman, S. C. Cramer, J. E. Bobrow, and D. J. Reinkensmeyer, "Automating Arm Movement Training Following Severe Stroke: Functional Exercises with Quantitative Feedback in a Gravity-Reduced Environment," *IEEE Transactions on Neural Systems and Rehabilitation Engineering*, vol. 14, no. 3, pp. 378-389, Sep. 2006.

[4] S. K. Banala, S. K. Agrawal, A. Fattah, V. Krishnamoorthy, W. L. Hsu, J. Scholz, and K. Rudlph, "Gravity-Balancing Leg Orthosis and Its Performance Evaluation," *IEEE Transactions on Robotics*, vol. 22, no. 6, pp. 1228-1239, Dec. 2006.

[5] S. K. Agrawal, S. K. Banala, A. Fattah, V. Sangwan, V, Krishnamoorthy, J. P. Scholz, and W. L. Hsu, "Assessment of Motion of a Swing Leg and Gait Rehabilitation With a Gravity Balancing Exoskeleton," *IEEE Transactions on Neural Systems and Rehabilitation Engineering*, vol. 15, no. 3, pp. 410-420, Sep. 2007.

[6] C. A. Oatis, *Kinesiology: The Mechanics & Pathomechanics of Human Movement, 1st ed.*, Philadelphia : Lippincott Williams & Wilkins, 2004.

[7] A. Gupta, M. K. O' Malley, "Design of a Haptic Arm Exoskeleton for Training and Rehabilitation," *IEEE Transactions on mechatronics*, vol. 11, no. 3, Jun. 2006.

[8] H. I. Krebs, N. Hogen, M. L. Aisen, B. T. Volpe, "Robot-Aided Neurorehabilitation," *IEEE Transactions on Rehabilitation Engineering*, vol. 6, no. 1, pp. 75-87, Mar. 1998.

[9] D. J. Reinkensmeyer, L. E. Kahn, M. Averbuch, A. McKenna-Cole, B. D. Schmit, W. Z. Rymer, "Understanding and treating arm movement impairment after chronic brain injury: Progress with the ARM guide," *Journal of Rehabilitation Research and Development*, vol. 37, no. 6, pp. 653-662, Nov/Dec 2000.

[10] J. C. Perry, J. Rosen, S. Burns, "Upper-Limb Powered Exoskeleton Design," *IEEE/ASME Transactions on mechatronics*, vol. 12, no. 4, pp. 408-417, Aug. 2007.

[11] M. J. French, M. B. Widden, "The Spring-and-lever Balancing Mechanism, George Carwardin and the Anglepoise lamp," *Proceedings of the Institution of Mechanical Engineers,* vol. 214(Part C), pp. 501-508, 2000.

[12] T. Rahman, R. Ramanathan, R. Seliktar, W. Harwin,

“A Simple Technique to Passively Gravity-Balance Articulated Mechanisms,” *ASME Journal of Mechanical Design*, vol. 117, no. 4, pp. 655-658, Dec. 1995.

[13] D. A. Streit, E. Shin, “Equilibrators for Planar Linkages,” *ASME Journal of Mechanical Design*, vol. 115, no. 3, pp. 604-611, Sep. 1993.

[14] L. E. Kahn, P. S. Lum, W. Z. Rymer, D. J. Reinkensmeyer, “Robot-assisted movement training for the stroke-impaired arm: Does it matter what the robot does?” *Journal of Rehabilitation Research & Development*, vol. 43, no. 5, pp. 619-630, Aug/Sep 2006.

[15] D. J. Magermans, E. K. J. Chadwick, H. E. J. Veeger, F. C. T. van der Helm, “Requirements for upper extremity motions during activities of daily living,” *Clinical Biomechanics*, vol. 20, no. 6, pp. 591-599, Jul. 2005.

[16] J. Rosen, J. C. Perry, N. Manning, S. Burns, B. Hannaford, “The human arm kinematics and dynamics during daily activities-Toward a 7 DOF upper limb powered exoskeleton,” in. *Proc. 12th Int. Conf. Adv. Robot.* (ICAR 2005), Jul., pp.532-539

[17] K. N. An, A. O. Browne, S. Korinek, S. Tanaka, B. F. Morrey, “Three-dimensional kinematics of glenohumeral elevation,” *Journal of Orthopaedic Research*, vol. 9, no. 1, pp. 143-149, Jan. 1991.

[18] H. Zhou, T. Stone, H. Hu, N. Harris, “Use of multiple wearable inertial sensors in upper limb motion tracking,” *Medical Engineering and Physics*, vol. 30, no. 1, pp. 123-133, Jan. 2008.

[19] T. M. Barker, A. C. Nicol, I. G. Kelly, J. P. Paul, “Three-dimensional joint co-ordination strategies of the upper limb during functional activities,” *Proceedings of the Institution of Mechanical Engineers, Part H: Journal of Engineering in Medicine*, vol. 210, no. 1, pp. 17-26, 1996.

[20] A. A. Hussein, C. Tarry, R. Datta, G. S. Mittal, M. Abderrahim, “Dynamic biomechanical model for assessing and monitoring robot-assisted upper-limb therapy,” *Journal of Rehabilitation & Development*, vol. 44, no. 1, pp. 43-62, 2007.

[21] NASA Reference Publication 1024, 1978, “Anthropometric Source Book: Volume I: Anthropometry for Designers,” NASA.

[22] R. F. Chandler, C. E. Clauser, J. P. McConville, H. M. Reynolds, J. W. Young, 1975, “Investigation of Inertia Properties of the Human Body, Final Report, Apr. 1, 1972 – Dec. 1974.” AMRL-TR-74-137, Aerospace Medical Research Laboratories, Wright-Patterson Air Force Base, Dayton, Ohio.

[23] C. E. Clauser, J. T. McConville, J. W. Young, 1969, “Weight, Volume and Center of Mass of Segmens of the Human Body.” AMRL-TR-69-70, Aerospace Medical Research Laboratories, Wright-Patterson Air Force Base, Dayton, Ohio. NASA CR-11262.

[24] P. S. Lum, C. G. Burgar, P. C. Shor, M. Majmunder, M. V. Loos, “Robot-Assisted Movement Training Compared With Conventional Therapy Techniques for the Rehabilitation of Upper-Limb Motor Function After Stroke,” *Archives of Physical Medicine and Rehabilitation*, vol. 83, pp. 952-959, Jul, 2002.

[25] Naval Biodynamics Laboratory, Mar. 1988, “Anthropometry and Mass Distribution for Human Analogues, Volume I: Military Male Aviators,” Naval Medical Research and Development Command Bethesda

被動式上肢復健訓練穿戴型機械手臂設計

林博揚[1]　謝文賓[2]　陳達仁[3]
[1]國立台灣大學機械工程系
[2]明志科技大學機械工程系
[3]國立台灣大學機械工程系暨工業工程研究所

本文提供一上肢穿戴式機械手臂(Exoskeleton)之設計用於中風患者或肌肉麻痺患者之上肢復健及訓練。此機構內含三個零自由長度彈簧可以平衡患者之上肢重量在其任意位置，提供了等效無重力場環境使患者可以自行進行復健動作及訓練。本設計不包含任何驅動器卻能達到類似於其他主動式物理治療機械手臂系統相同之功能，是較為經濟及簡單的設計。本設計之模擬模型已建構於 ADAMS 中，根據模擬上肢日常生活動作(Activities of daily livings)作為測試，結果證實可以有效達到重力平衡的效果，並探討本設計對於上肢參數估計誤差於平衡效果影響之可靠度。

關鍵詞: 上肢復健，重力平衡，機械手臂式物理治療，彈簧平衡。